"Intrinsic" and "Topological" Stiffness in Branched Polymers

Ronan Connolly,[†] Giovanni Bellesia,[†] Edward G. Timoshenko,[*,†,‡] Yuri A. Kuznetsov,[§] Stefano Elli,[||] and Fabio Ganazzoli[||]

Theory and Computation Group, Department of Chemistry, Centre for Synthesis and Chemical Biology, Conway Institute of Biomolecular and Biomedical Research and Computing Centre, University College Dublin, Belfield, Dublin 4, Ireland, and Dipartimento di Chimica, Materiali e Ingegneria Chimica "G. Natta", Sez. Chimica, Politecnico di Milano, via L. Mancinelli 7, 20121 Milano, Italy

Received November 5, 2004; Revised Manuscript Received April 13, 2005

ABSTRACT: Single-chain Monte Carlo simulations were carried out, in continuous space, of polymers with various topologies (branched and linear) in the good solvent. Using an inherently flexible bead-and-spring model, the backbone of linear polymers with either linear or dendritic side-groups attached was found to be elongated, indicative of an induced stiffness. This "topological stiffness" was compared to the "intrinsic stiffness" of semiflexible linear polymers in terms of various observables. Semiflexible comb polymers, which contained both types of stiffness, were also considered.

1. Introduction

Even early simulations of comb-branched polymers in good solvent have indicated that the backbones of these polymers tend to be stretched compared to their linear counterparts.[1] This stretching is widely accepted to be due to steric repulsion between the side-chains. To minimize this repulsion, comb-branched polymers seem to adopt conformations in which the backbone is slightly elongated compared to the coillike conformations of flexible linear polymers. This elongation increases the separation between side-chains, although it does involve a loss in conformational entropy for the backbone.

Actually, when the backbone is relatively short, comb-branched polymers may adopt starlike conformations wherein the side-chains are able to "wrap" around the flexible backbone without too much repulsion between side-chains.[2] However, when the degree of polymerization of the backbone is increased, elongation becomes preferable. This phenomenon of elongation has been treated theoretically by Denesyuk[3] for the related brush polymers. In the latter, star polymers are grafted onto the backbone instead of linear side-chains. The backbone stretching results in its certain rigidity, even for intrinsically flexible polymers. This stiffness can be distinguished from the "intrinsic" stiffness that all polymers have at an atomistic level because of the bonded interactions because it depends on the topology of the polymer, and thus it is referred to as the "topological" stiffness.

The intrinsic stiffness of linear polymers, usually discussed in terms of the persistence length, l_p, and the Kuhn segment length, l_K, is discussed in many standard books on polymers.[4−6] However, often the stiffness that is experimentally determinable[6,7] also contains contributions from factors other than the intrinsic stiffness. One example is the repulsive excluded volume interactions that even linear polymers demonstrate when in good solvents.[8,9] This is the contribution that makes linear chains "self-avoiding" in a good solvent. We will refer to it as the "linear chain excluded volume contribution" (LCEVC). While the intrinsic stiffness, in effect, acts purely through the connectivity of the polymer, the excluded volume contribution acts through three-dimensional (3D) space, although it is also strongly affected by the connectivity.[8] Recent years have also seen an interest in understanding the contribution of the "electrostatic" stiffness because of the Coulombic repulsion between like charges for polyelectrolytes.[10−12] In addition to the intrinsic stiffness and LCEVC, comb-branched polymers appear to have an additional topological stiffness contribution, as previously mentioned, which is similar in origin to the LCEVC although, in the branched polymers studied here, the LCEVC term is typically smaller in magnitude.

Because of the synthesis of high-density comb polymers, the topological stiffness of the backbones of comb-branched and related polymers has become increasingly relevant. For instance, in 1989, Tsukahara et al. successfully polymerized methacryloyl end-functionalized polystyrene macromonomers with extremely high degrees of polymerization ($D_P \approx 1000$).[13] "Poly(macromonomer)s" such as these can be considered as comb-branched polymers, where each monomer in the backbone contains a side-chain. They were analyzed extensively in terms of viscosity measurements, X-ray scattering, light scattering, scanning force microscopy (SFM), small angle neutron scattering (SANS), and GPC/MALLS by the groups of Tsukahara, Schmidt, and others,[14] and it was found that the backbones adopted stiff, almost rodlike conformations, as indicated by the measured Kuhn length of $l_K > 1000$ Å. This extended structure of the backbone has been attributed to a topological stiffness caused by the extensive overcrowding of the side-chains, which are only separated by a contour length of $l = 2.5$ Å along the backbone. The side-chains themselves are moderately long, meaning that

* Author to whom correspondence should be addressed. E-mail: Edward.Timoshenko@ucd.ie. Web page: http://darkstar.ucd.ie.
[†] Theory and Computation Group, Department of Chemistry University College Dublin.
[‡] Centre for Synthesis and Chemical Biology, Conway Institute of Biomolecular and Biomedical Research, University College Dublin.
[§] Computing Centre, University College Dublin.
[||] Politecnico di Milano.

10.1021/ma0477246 CCC: $30.25
Published on Web 05/17/2005

these polymers adopt curved cylindrical conformations with diameters of, e.g., $d \approx 70-150$ Å, leading to their description as "molecular bottlebrushes".[13−15]

A similar phenomenon to the induced rigidity of the backbones of these comb polymers has been observed experimentally for another recently synthesized type of polymer, which we will call "poly(dendron)s". These polymers comprise a linear "backbone", with numerous side-groups attached, which are dendritic in nature, i.e., highly branched.[16,18−28]

Poly(dendron)s are related to the relatively modern class of polymers called dendrimers.[29] Dendrimers typically comprise a core focal point to which several (typically two to four) "dendrons" (regularly branched groups in which each "generation" of branching involves introducing a new branch point to every unbranched branch) are attached. Poly(dendron)s have a linear backbone to which the dendrons are attached instead of a single core molecule. Hence, we will use the term poly(dendron) to describe these polymers, as has also been used by Kaneko et al.[16] It should be noted, however, that there are currently many different names used in the literature for these polymers,[17] e.g., dendronized (linear) -polymers,[18−20] monodendron-jacketed linear polymers,[21] side-chain dendritic polymers,[22] architectural copolymers,[23] wormlike dendrimers,[24] or rodlike dendrimers.[25]

Much of the work on these polymers is still on synthetic approaches. However, many groups are now beginning to evaluate their properties.[19,21,22,26,27] Current experimental results and synthetic approaches have been reviewed in several recent articles.[20] The most striking observation is the rigidity of the backbones, which can be pronounced enough to allow direct observation when adsorbed on a surface via, e.g., SFM.[21,26] Rigidity has also been observed in solution via SANS.[26,27] Presumably, this stiffening of the backbone of these poly(dendron)s is another example of a topological stiffness. However, despite the experimental evidence, any rigorous evaluation of these systems by either theory or simulation is currently limited to a recent study by Christopoulos et al.[19]

In contrast, the poly(macromonomer) systems have been widely studied by both theory[3,30,31,38] and simulations.[32−38] Most of these studies have used a flexible model for both the backbone and the side-chains,[3,30,32−35] although recent studies have considered the cases of semiflexible backbones with flexible side-chains,[31] flexible backbones with semiflexible side-chains,[37] and semiflexible backbones with rigid side-chains.[38] The use of a flexible model assumes that the stiffness induced by the presence of side-chains can be distinguished from the intrinsic stiffness of the polymer. However, it should be noted that even linear polymers that are intrinsically flexible show a persistence of length in the good solvent.[8] Unfortunately, until now, there does not appear to have been any attempt to directly compare the intrinsic and topological types of stiffness, which we shall attempt in this paper for different systems. With this in mind, the stiffness of the backbones of intrinsically flexible poly(macromonomer)s and poly(dendron)s will be compared to the stiffness of linear, semiflexible polymers of the same length via Monte Carlo simulation data. To evaluate how the intrinsic stiffness modifies the topological stiffness, we will also consider poly(macromonomer)s with semiflexible backbones.

2. Technical Details and Nomenclature

The results reported in this paper have been obtained via coarse-grained Monte Carlo simulations on the basis of the Metropolis algorithm[39] in continuous space, as it has been previously used by our group to describe various different branched and/or semiflexible topologies, and we refer the interested reader to refs 32,40, and 41 (and references therein) for further technical details.

We describe the potential energy of our systems via the following Hamiltonian:

$$\frac{H}{k_B T} = \frac{1}{2l^2}\sum_{i\sim j}\kappa_{ij}(\mathbf{X}_i - \mathbf{X}_j)^2 + \frac{1}{2l^2}\sum_{i\approx j\approx k}\lambda_{ijk}(\mathbf{X}_i + \mathbf{X}_k - 2\mathbf{X}_j)^2 + \frac{1}{2}\sum_{ij,i\neq j}U_{ij}^{(HC)}(|\mathbf{X}_i - \mathbf{X}_j|) \quad (1)$$

where $\mathbf{X}_i$ are the monomer coordinates and l is the characteristic bond length. Here, κ_{ij} and λ_{ijk} are the constants that are predefined at the start of a simulation.

The first term represents the connectivity of the polymer with harmonic springs of nonzero strength κ_{ij} introduced between any unique pair of connected monomers (which we denote by $i\sim j$). We define here $\kappa_{ij} \equiv 3$ for all bonded pairs, for easy comparison with the standard Edwards model[5] of a Gaussian chain.

We model the intrinsic stiffness of the polymers via the second term, which involves the square of the discretised local curvature of the chain, as defined in the Frenet−Serret basis, although our definition differs in the normalization factor.[42] It should be noted that, for our systems, the λ_{ijk} constants may be nonzero only between two consecutive bonds ($i \approx j \approx k$). Increasing these nonzero λ_{ijk} values increases the intrinsic stiffness of the polymers. However, if $\lambda_{ijk} = 0$, this corresponds to an intrinsically flexible model.

For most of this paper, we will treat our *branched* systems with $\lambda_{ijk} = 0$ so that any rigidity they may demonstrate will be entirely due to excluded volume effects. For comparison, we will also report results from *linear* polymers with increasing λ_{ijk}. It should be noted that when $\lambda_{ijk} = 0$, the diameter, d, of a "monomer" is comparable to the intrinsic Kuhn length of the polymer in an ideal solution. Finally, we will discuss some representative branched systems with increasing λ_{ijk} in the backbone. These systems will hence possess both intrinsic and topological stiffness (as well as LCEVC).

The excluded volume effects are modeled via a hard-core potential term, $U_{ij}^{(HC)}(|\mathbf{X}_i - \mathbf{X}_j|)$, in the potential, defined as zero if $|\mathbf{X}_i - \mathbf{X}_j| > d$ and infinity otherwise. Hence, these polymers can be described as being in the good, athermal solvent. For convenience, we describe all lengths in terms of the monomer diameter, which we define as $d = l \equiv 1$, and energies in units of $k_B T$.

For consistency, in this study, the degree of polymerization of all of the linear polymers is $N = 48$, and the number of monomers in the backbones, N_b, of all of the branched polymers is also $N_b = 48$. This is a relatively short length for the simpler topologies such as the linear chains, but the systems can become quite large for the chains with bulky side-groups, which are the main interest here.

For the branched polymers, the number of spacers, S, between each side-group along the backbone ranged

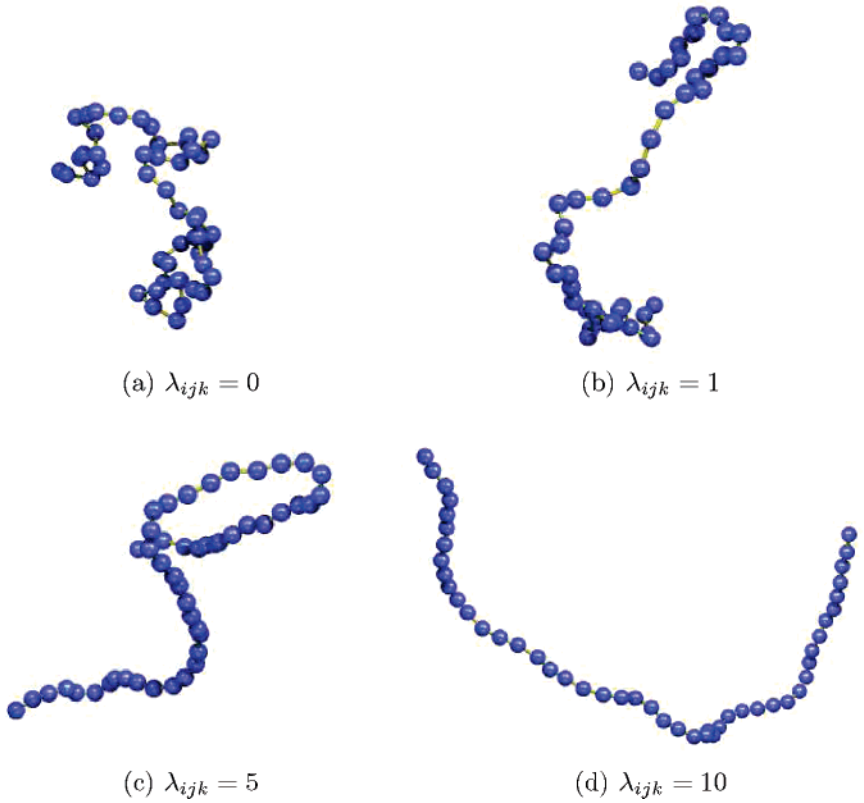

Figure 1. Typical snapshots, from Monte Carlo simulations, of linear polymers (48 monomers long) in the good solvent with increasing bending penalty constants (λ_{ijk} in eq 1). $\lambda_{ijk} = 0$ corresponds to the intrinsically flexible case, while larger values correspond to an increasing intrinsic rigidity of the polymer. Unless specifically stated, the diameter of the spheres in all the snapshots reported in this paper correspond to the excluded volume diameter of the monomer beads, d.

from 0 to 3 monomers. We considered systems where the first monomer in the backbone has a side-group. However, this means that the last S monomers of the backbone are left bare, and so it is possible to compare bare end monomers and end monomers with side-groups by comparing the "first" and "last" monomers. For the comb polymers, the length of the arms, N_a, was either 5 or 10 monomers. The dendrons of the poly(dendron)s are denoted by D, the number of monomers before a branch point, and G, the number of generations of branching, using the same nomenclature that we have previously used for dendrimers.[40]

Linear polymers with different flexibilities were considered by changing the bending penalty constants, λ_{ijk}, in the range 0 (flexible)...5, 10 (semiflexible).

Finally, to illustrate the effects of combining both intrinsic and topological stiffness, comb polymers were also considered with semiflexible backbones. For these polymers, the arms were flexible and of length $N_a = 5$. The bending penalty of the monomers in the backbone was $\lambda_{ijk} = 0 \ldots 3, 5, 10$.

3. Results

Snapshots taken from equilibrated MC simulations of linear polymers with various bending penalties are illustrated in Figure 1, while snapshots for various intrinsically flexible, branched polymers are illustrated in Figure 2. One can obtain a simplistic, yet qualitative understanding of the systems studied in this paper from these figures. In Figure 1, one can see that increasing λ_{ijk} does indeed reduce the number of sharp bends along the chain, and hence makes the chain "straighter" with a greater correlation between consecutive monomers along the chain, i.e., a greater persistence length. For the branched polymers illustrated in Figure 2, it can be seen that the elongation of the backbone arises in an attempt to minimize the steric congestion between the side-groups and that this elongation becomes more pronounced the greater the congestion is, e.g., the backbone of the $S = 0$, D4G2 poly(dendron) in Figure 2f appears more elongated than the backbone of the $S = 0$, D1G2 poly(dendron) in Figure 2d. Obviously, increasing the distance between side-groups along the backbone, i.e., S, reduces this congestion, as can be seen by comparing, e.g., the comb polymers in Figure 2a and b or the poly(dendron)s in Figure 2e and f (D1G4 and D4G2 dendrons are similar in size, and hence degree of congestion). We note that Christopoulos et al. found that increasing the generation to G = 5 increased the steric congestion to such an extent that buckling of the backbone began to diminish its elongation.[19] We did not observe this phenomenon, although we only studied up to G = 4. However, the model used by Christopoulos et al. had fixed bond lengths, while our model (eq 1) does allow some bond stretching. This model therefore involves an additional method to diminish the congestion.

3.1. Static Structure Factors. The static structure factor is a useful observable, because it can be readily obtained from light and neutron scattering techniques.[6] Moreover, by selective deuteration, it is possible to obtain the partial structure factors of the backbone from SANS experiments. Indeed, Lecommandoux et al. have done this for poly(chlorovinyl ether) comb polymers with polystyrene side-chains.[14]

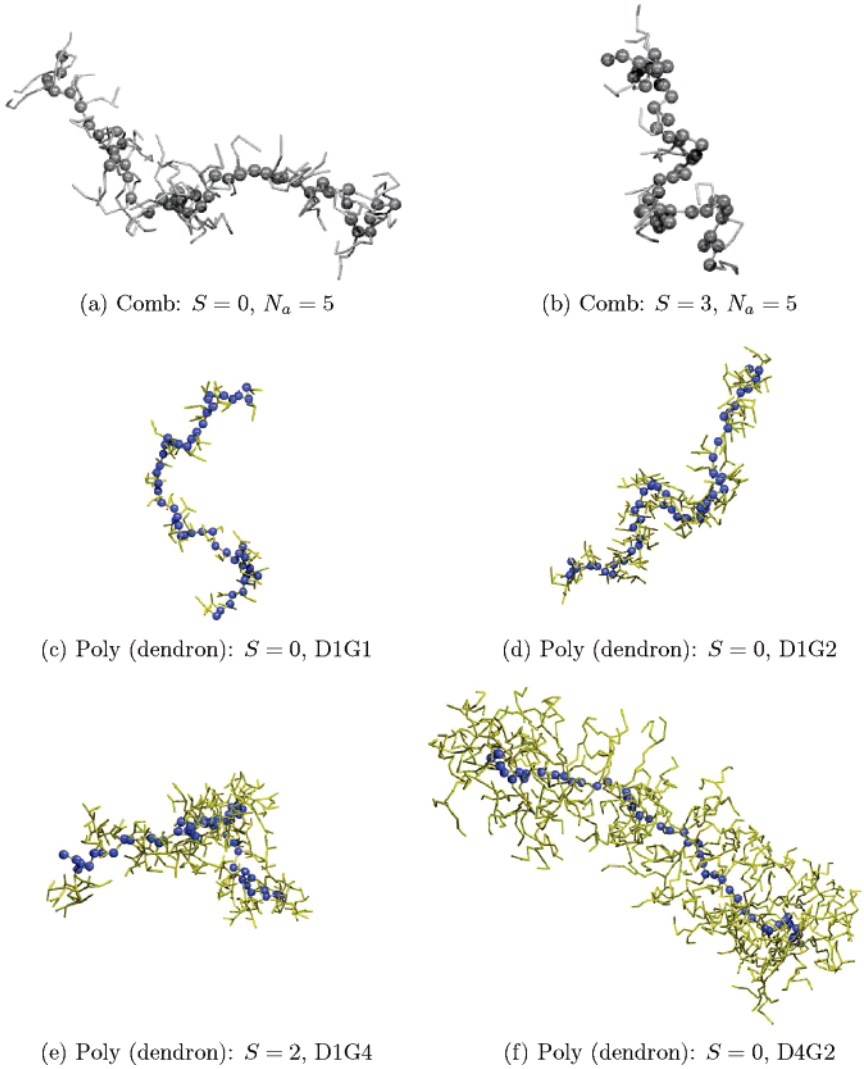

(a) Comb: $S = 0$, $N_a = 5$ (b) Comb: $S = 3$, $N_a = 5$

(c) Poly (dendron): $S = 0$, D1G1 (d) Poly (dendron): $S = 0$, D1G2

(e) Poly (dendron): $S = 2$, D1G4 (f) Poly (dendron): $S = 0$, D4G2

Figure 2. Typical snapshots, from Monte Carlo simulations, of various comb polymers and poly(dendron)s (see the legend) with the backbones 48 monomers long in the good solvent. The spheres of the side-groups are hidden here for visual clarity of the backbone.

The static structure factor (SSF), $S(q)$, is defined as follows:

$$S(q) = \frac{1}{N}\sum_{ij} \tilde{g}_{ij}^{(2)}(|\boldsymbol{q}|) \tag{2}$$

$$\tilde{g}_{ij}^{(2)}(\boldsymbol{q}) = \langle \exp(i\boldsymbol{q}(\mathbf{X}_i - \mathbf{X}_j))\rangle = \frac{1}{2\pi^2}\int_0^\infty r^2\, \mathrm{d}r\, \frac{\sin(qr)}{qr} g_{ij}^{(2)}(r) \tag{3}$$

where tilde indicates the 3D Fourier transform, q is the scattering momentum or wavenumber,

$$q = \frac{4\pi \sin\left(\frac{\theta}{2}\right)}{\lambda} \tag{4}$$

and $g_{ij}^{(2)}(r)$ is the monomer−monomer radial distribution function,

$$g_{ij}^{(2)}(\boldsymbol{r}) \equiv \langle \delta(\mathbf{X}_i - \mathbf{X}_j - \mathbf{r})\rangle = \frac{1}{4\pi r^2}\langle \delta(|\mathbf{X}_i - \mathbf{X}_j| - r)\rangle \tag{5}$$

It is convenient to report static structure factors using rescaled Holtzer forms,

$$\hat{S}(\hat{q}) = \frac{q\sqrt{R_g^2}}{N} S(q), \quad \hat{q} = q\sqrt{R_g^2} \tag{6}$$

In Figures3 and 4, we present SSFs of the various systems from this study in the Holtzer form. One can say that $1/q$ corresponds to the "probing distance", where q is the scattering vector length, i.e., the scattering $S(q)$ is predominantly due to correlated particles at a distance $1/q$.[6] The Holtzer forms are relevant here because $S(q) \propto q^{-1/\nu}$ for large q, and in particular, $S(q) \propto q^{-1}$ when $ql_p > 1$, where l_p is the persistence length because on these length scales, the polymer behaves as a rigid rod with $\nu = 1$. Hence, by plotting $q \cdot S(q)$ against q, i.e., using Holtzer plots, a plateau should be reached at the persistence length. One should realize, however, that the scattering data obtained from these simulations is basically meaningless for length scales smaller than the monomer diameter, i.e., when about $\hat{q} \geq 2\pi$.

In Figure 3a, a complete plateau is only observed for the most rigid of the semiflexible polymers, where $\lambda_{ijk} = 10$. For large values of $\hat{q}$, the comb backbones appear better modeled as semiflexible polymers. Indeed, as the

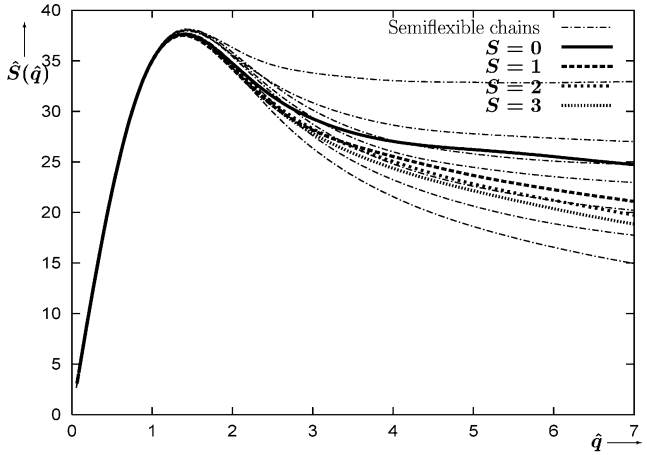

(a) Varying number of spacers

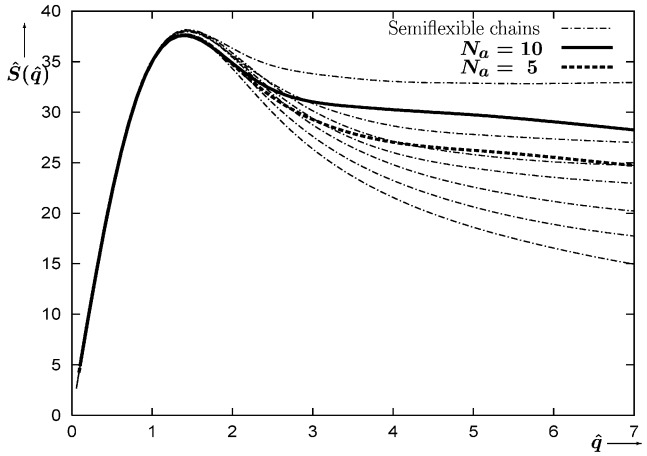

(b) Varying arm length

Figure 3. Comparison of the rescaled static structure factors, $\hat{S}(\hat{q})$, of the backbones of various comb polymers against those for various semiflexible linear polymers, obtained from MC simulation results. The lengths of all the backbones and linear polymers were 48 monomers. The dash−dotted lines correspond to linear polymers with bending penalties of $\lambda_{ijk} = 0$, 1, 2, 3, 4, 5, 10 (from bottom to top). The relative statistical errors of all the $\hat{S}(\hat{q})$ plots reported in this paper are smaller than resolution can distinguish because of the extensive averaging inherent in the function and so are not included. (a) Side-chains of the combs were 5 monomers long. The labeled lines correspond to scattering curves for backbones with spacers of $S = 0...3$ (top to bottom). (b) Side-chains of the combs were either 5 or 10 monomers long, but there were no spacers along the backbone, i.e., $S = 0$.

number of spacers, S, is reduced, the backbones are modeled better by polymers with increasing values of λ, suggesting an increase in the overall stiffness of the polymer. However, for smaller values of $\hat{q}$, the backbones seem better modeled as flexible polymers. This indicates a substantially different scattering behavior for intrinsically stiff and topologically stiff polymers, which should be experimentally observable.

In Figure 3b, we can see that increasing N_a increases the scattering for larger $\hat{q}$ values ($3 \leq \hat{q} \leq 7$), as does increasing λ_{ijk}, suggesting that increasing N_a does indeed increase the stiffness (although there has been some discussion as to the possibility that the increase in stiffness with increasing N_a is quickly saturated[30,34,35]). However, for both polymers, there does seem to be a slight oscillatory behavior, which does not occur for the linear cases, the origin of which is not clear yet.

In Figure 4, poly(dendron)s of increasing generation, with $S = 0$, are considered. It can be seen that the D1G3 and D1G4 plots seem to reach plateau values, indicative of a strong rigidity. However, again, the plots are substantially different from the plots for linear polymers, suggesting an experimentally achievable approach to comparing the intrinsic stiffness of semiflexible, linear chains to the topological stiffness of poly(dendron)s.

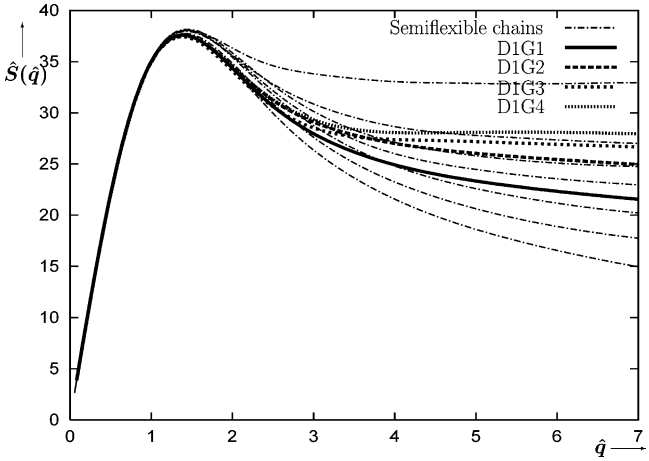

Figure 4. Comparison of the rescaled static structure factors, $\hat{S}(\hat{q})$, of the backbones of various poly(dendron)s of increasing generation against those for various semiflexible linear polymers, as in Figure 3. The number of spacers between dendrons along the backbone was $S = 0$.

3.2. Correlation Function Plots. Although useful for comparing simulations with experimental data, the SSFs are quite complex in interpretation and not very intuitive. Fortunately, there are more intuitive observables that can be calculated from simulation data. We will consider two of these widely used observables in this paper, the first of which is the correlation function of the bond angles formed by the backbone as a function of their topological separation,

$$\langle \cos \theta(s) \rangle = \left\langle \frac{1}{N-1-s} \sum_{i=1}^{N-1-s} \vec{u}_i \cdot \vec{u}_{i+s} \right\rangle \qquad (7)$$

where $s \in [0, N-2]$ is the separation (in number of bonds) along the backbone, and $\vec{u}_i \equiv \vec{r}_i/|\vec{r}_i|$ is the normalized bond vector between monomer i and monomer $i+1$. Hence, by definition, the correlation for $s = 0$, i.e., the self-term, is exactly unity: $\langle \cos \theta(0) \rangle \equiv 1$. For a truly random walk, consecutive vectors are completely uncorrelated, and hence $\langle \cos \theta(s > 0) \rangle = 0$, i.e., all directions are equally probable. In contrast, for a completely rigid rod, all vectors have the same direction and $\langle \cos \theta(s > 0) \rangle = 1$. For a semirigid polymer, the correlation should fall from one to zero with increasing separation, and a definition for the persistence length can be obtained from the rate of this decay.[4−6] For a Kratky−Porod "wormlike chain",[4,43] the decay is strictly exponential in nature,[4]

$$\langle \cos \theta(s) \rangle = \exp\left(\frac{-s}{\tau}\right) \qquad (8)$$

where τ is the Kratky−Porod persistence length.[4]

With this in mind, the $\langle \cos \theta(s) \rangle$ data for the semiflexible, linear polymers were fitted to eq 8 in Figure 5. The Kratky−Porod model provided reasonable fits for the polymers with larger bending penalties, e.g., $\lambda_{ijk} \geq 4$. However, for smaller values of λ_{ijk}, the decay in $\langle \cos \theta(s) \rangle$ for large values of s did appear to be slower than

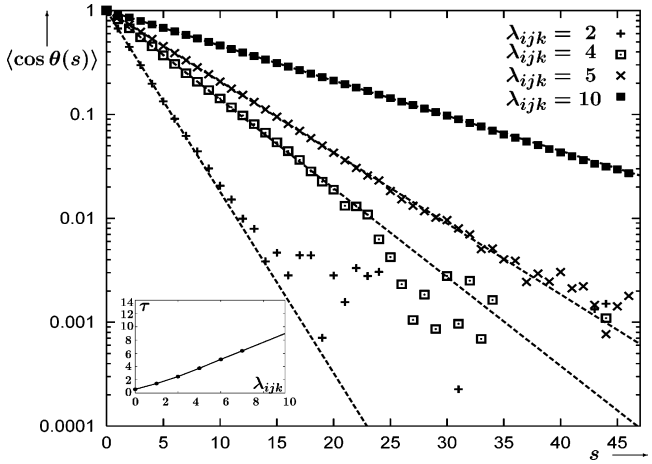

Figure 5. Attempts to fit $\langle \cos \theta(s) \rangle$ for several semiflexible, linear polymers ($\lambda_{ijk} = 2, 4, 5, 10$) to the Kratky−Porod model via eq 8. The dashed lines correspond to the obtained fittings. The values of τ obtained from the fittings of these (and other values of λ_{ijk}) are plotted in the inset with respect to the bending penalty, λ_{ijk}.

a fitted exponential one, suggesting the Kratky−Porod model is only accurate for the more intrinsically rigid polymers. The relationship between λ_{ijk} and τ is reported in the inset of Figure 5. It is interesting to note that in the intrinsically totally flexible case ($\lambda_{ijk} = 0$), $\tau = 0.569 \pm 0.017 > 0$. This is due to the LCEVC discussed in Section 1 and agrees with Schäfer and Elsner's observation that intrinsically flexible linear polymers do have a significant persistence length in the good solvent.[8]

We should note that the data for larger values of s do appear noisier, which is understandable because the degree of averaging is smaller in eq 7 and also the degree of precision required is correspondingly higher for the smaller values of $\langle \cos \theta(s) \rangle$ on these log-linear plots, although exact values for the error bars are more difficult to estimate.

Attempts to apply the Kratky−Porod model to the backbones of comb polymers have been carried out by Saariaho et al.[33−35] and also recently by our group.[32] Figure 6 plots further attempts to apply this model to the backbones of both comb polymers and poly(dendron)s. Although the standard exponential equation did not provide good fits, if one excluded the first few values of s ($s \leq 3$) from the fitting, one could obtain reasonable fits by the following equation:

$$\langle \cos \theta(s) \rangle = a \exp\left(\frac{-s}{\tau}\right) \tag{9}$$

where $0 < a < 1$ is the y-intercept.

The problem with this fitting is that if one extrapolates the model to $s = 0$, a value of $\langle \cos \theta(s) \rangle$ is obtained which is less than one, i.e., a. This disagrees with the earlier statement that $\langle \cos \theta(0) \rangle \equiv 1$. Attempts have been made to explain this discrepancy in terms of different "characteristic length scales".[33−35] Saariaho et al. suggested that the backbone of these systems may be rather flexible at small length scales and become extended on a larger length scale only. They suggest that this explains the strong decline in $\langle \cos \theta(s) \rangle$ for small values of s,[33] which they claim represents the local small length scale flexibility of the backbone. However, in this context, we should note that both eqs 8 and 9 assume that the stiffness along the chain is uniform. While the assumption of a uniform stiffness is a valid

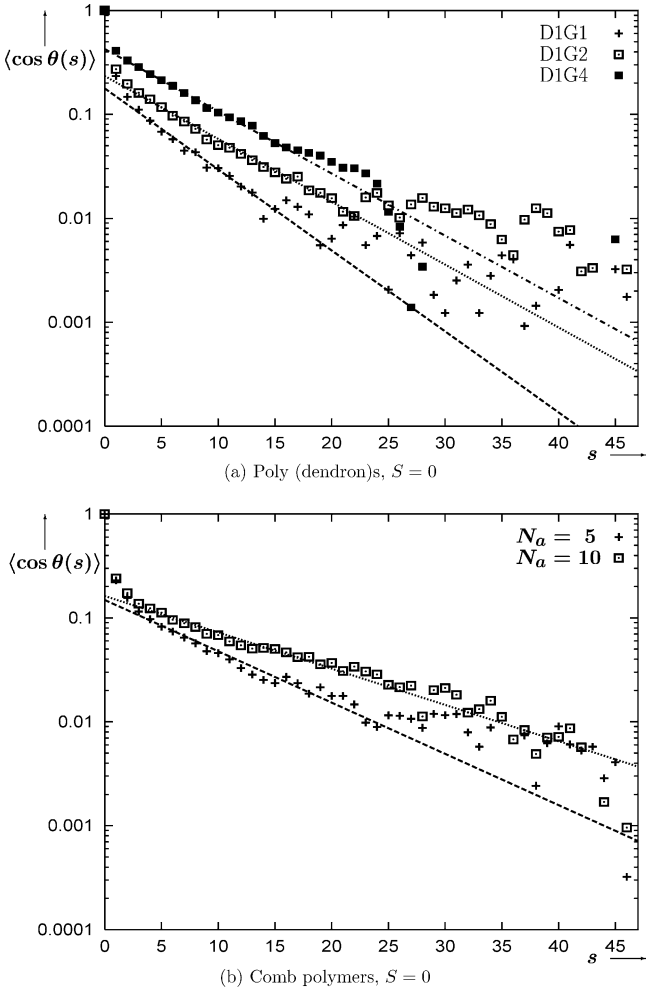

Figure 6. Attempts to fit $\langle \cos \theta(s) \rangle$ for various (a) poly(dendron)s and (b) comb polymers via eq 9. The dashed lines correspond to the obtained fittings.

one for the Kratky−Porod wormlike chains, the branched and linear chains studied here do not have a uniform stiffness along the length of the chain, e.g., "end effects" are obviously less evident in the middle of the chain! However, the definition of $\langle \cos \theta(s) \rangle$ treats, for example, the end and middle vectors as contributing equally to the mean values. The polymers with large bending penalties, e.g., $\lambda_{ijk} = 5$ or 10, should have a more uniform stiffness, and perhaps this is why they are better described by the exponential equation of the Kratky−Porod model. To remove the contribution of the "end effects" from $\langle \cos \theta(s) \rangle$, one *could* neglect the contribution of the end vectors to eq 7. However, again, this would assume that the rest of the chain demonstrates a uniform stiffness, which is not always the case, as will be later illustrated for branched polymers. Hence, for the rest of this paper, we will consider another observable that can illustrate the dependence on position within the chain.

3.3. Persistence Length Plots. The other observable we shall consider in this paper gives another definition of the persistence length attributable to Flory, through the projection of the end-to-end vector, $\vec{R}_b$, on the segment vector $\vec{r}_k$:

$$\langle l_p^{(k)} \rangle \equiv \left\langle \frac{\vec{r}_k}{|\vec{r}_k|} \cdot \vec{R}_b \right\rangle \tag{10}$$

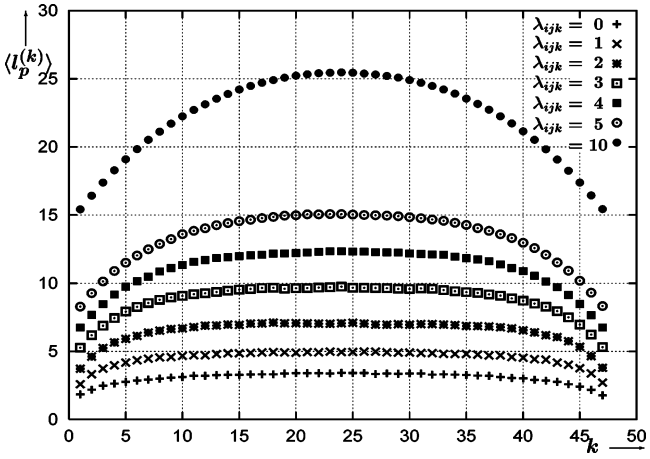

Figure 7. The persistence length plots, $\langle l_p^{(k)} \rangle$, obtained via eq 10, versus segment number, k, for various semiflexible, linear polymers, each of length 48. The strength of the intrinsic stiffness is varied between polymers by increasing the strength of the bending penalty, λ_{ijk} from 0 (bottom)...5, 10 (top).

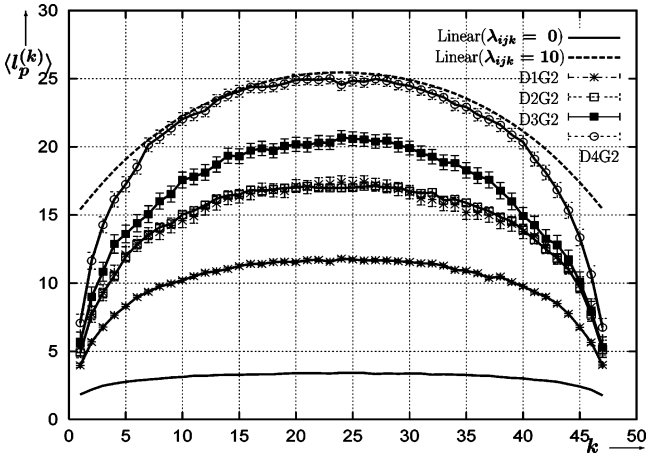

Figure 8. The persistence length plots, $\langle l_p^{(k)} \rangle$, versus segment number, k, as in Figure 7 for various poly(dendron)s with increasing number of spacers, D, within the dendrons. For comparison, the persistence length plot for a linear, flexible polymer, and a linear, semirigid ($\lambda = 10$) polymer with the same number of monomers as in the backbone of the poly(dendron)s is included.

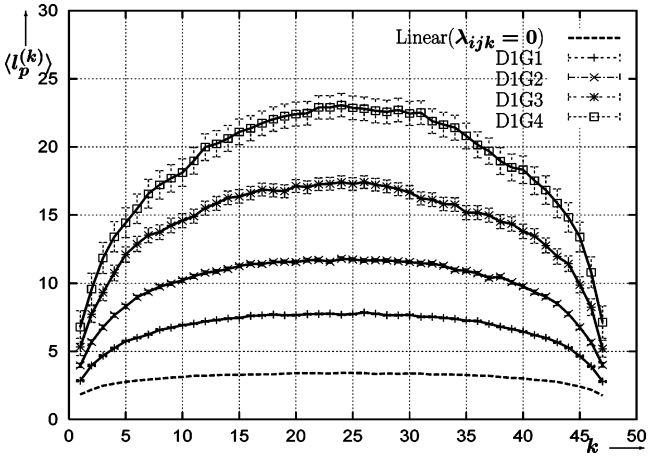

Figure 9. The persistence length plots, $\langle l_p^{(k)} \rangle$, versus segment number, k, as in Figure 7 for various poly(dendron)s with increasing generation number, G. For comparison, the persistence length plot for a linear, flexible polymer with the same number of monomers as in the backbone of the poly(dendron)s is included.

$\langle l_p^{(1)} \rangle$, i.e., the projection onto the first segment, is the definition typically used to describe the persistence length.[4] However, $\langle l_p^{(k)} \rangle$ has been found to depend strongly on k,[8,32] and so plots are reported here for the whole range of $1 \leq k \leq 47$.

The persistence length plots for linear polymers with various different bending penalties are reported in Figure 7. As has been previously noted,[32] the free ends of the polymers have a greater freedom, hence reducing the $\langle l_p^{(k)} \rangle$ values for small values of k and $N - k$. However, the plateau for intermediate values of k that occurs for small values of λ_{ijk} is less evident for increasing values of λ_{ijk} and, indeed, is not present at all for $\lambda_{ijk} = 10$. This may be because the chains considered here are not sufficiently long ($N = 48$ monomers) for the plateau to develop for the more rigid chains, but this issue could only be resolved by studies of much larger systems.

It can be seen that increasing the bending penalty increases the rigidity of all parts of the chain substantially, e.g., $\langle l_p^{(1)} \rangle$ for the $\lambda_{ijk} = 10$ case is still comparable to the maximum $\langle l_p^{(k)} \rangle$ value for the $\lambda_{ijk} = 5$ case. However, topological stiffness appears to have a different behavior for the $\langle l_p^{(k)} \rangle$ plots, as can be seen in Figure 8, where poly(dendron)s with dendrons of different size (and hence steric congestion) are compared. For intermediate values of k, the plots of the topologically stiff backbones and the intrinsically stiff polymers are quite similar, e.g., the D4G2 case is quite similar to the $\lambda_{ijk} = 10$ case for $8 \leq k \leq 39$. However, for small values of k and $N - k$, the $\langle l_p^{(k)} \rangle$ values are substantially diminished for the poly(dendron)s compared to the semiflexible, linear polymers. This suggests that the end effects are more significant for topological stiffness than for intrinsic stiffness, which is significant experimentally. For instance, this may explain the experimental observation that short comb polymers behave more like star polymers than "bottlebrushes",[2] i.e., the backbones of short comb polymers are relatively flexible. This can also be qualitatively seen by considering the relatively flexible end-groups of the D4G2 polydendron illustrated in Figure 2f.

Figure 9 illustrates the $\langle l_p^{(k)} \rangle$ plots for increasing generations of branching of the dendrons (D = 1 and $S = 0$). Increasing the number of generations increases the stiffness of the backbones in a manner similar to increasing the number of spacers, D, within the dendrons. This is to be expected because increasing either term increases the steric congestion caused by the dendrons. It can be seen that for all of these examples of topologically stiff polymers (Figures 8 and 9, as well as Figures 10 and 11, which we shall discuss shortly), the $\langle l_p^{(k)} \rangle$ values are larger than in the case of the $\lambda_{ijk} = 0$ linear flexible chain in Figure 7. However, it is important to realize that this topological stiffness is most pronounced on the monomers directly connected to the side-groups. This can be seen in Figures 10 and 11, where we consider the effects on increasing the number of spacers between the side-chains along the backbone, S, for D1G3 poly(dendron)s (Figure 10) and combs with $N_a = 10$ (Figure 11a) and $N_a = 5$ (Figure 11b). First, it can be seen that increasing S decreases the overall topological stiffness. This is not surprising because the relative concentration of the bulky side-chains is reduced, lowering the amount of steric conges-

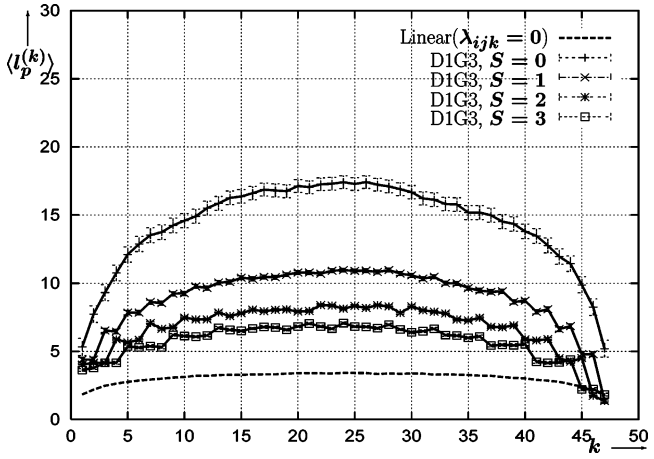

Figure 10. The persistence length plots, $\langle l_p^{(k)} \rangle$, versus segment number, k, as in Figure 7 for various D1G3 poly(dendron)s with different numbers of backbone spacers, S. For comparison, the persistence length plot for a linear, flexible polymer with the same number of monomers as in the backbone of the poly(dendron)s is included.

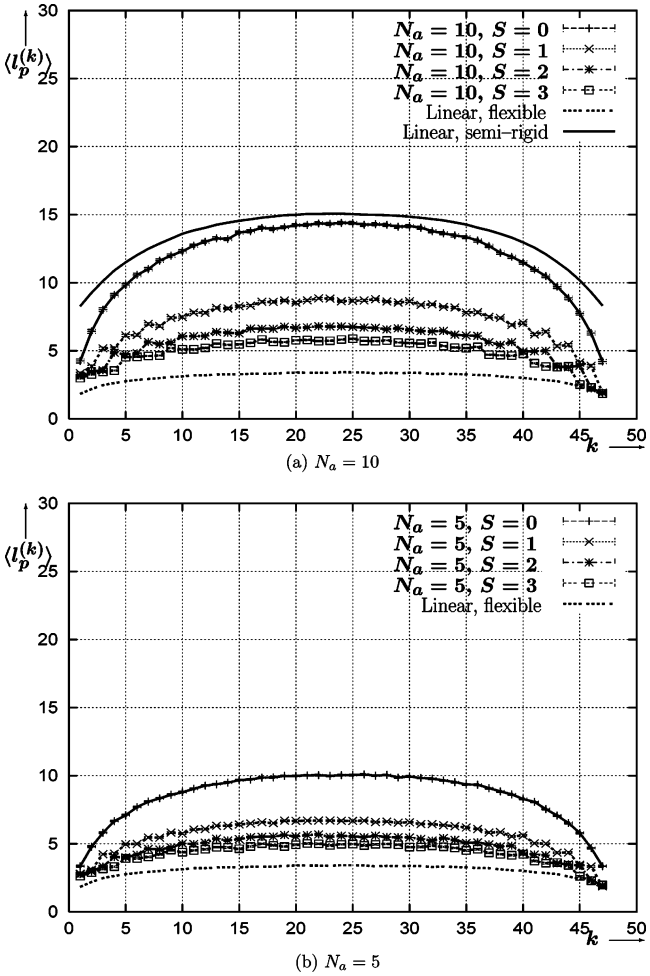

Figure 11. The persistence length plots, $\langle l_p^{(k)} \rangle$, versus segment number, k, as in Figure 10 for comb polymers with (a) $N_a = 10$ and (b) $N_a = 5$ and different numbers of spacers between the side-chains along the backbone. For comparison, the persistence length plot for a linear, flexible polymer, and a linear, semirigid ($\lambda = 5$) polymer with the same number of monomers as in the backbone of the poly(dendron)s is included.

tion they cause. Second, we notice that increasing S introduces a steplike phenomenon to the $\langle l_p^{(k)} \rangle$ plots, especially pronounced for small values of k and $N - k$. The monomers that are directly connected to the side-chains are more restricted than that of their neighboring monomers. Hence, for every $S + 1$ monomers, there is an increase in $\langle l_p^{(k)} \rangle$. It should be noted that, although $\langle l_p^{(k)} \rangle$ is larger for monomer bonds directly connected to side-chains, the side-chains also affect the neighboring monomers because their $\langle l_p^{(k)} \rangle$ values are larger than that of their linear, flexible chain counterparts, even for $S = 3$. The exception to this are the last S bonds, which have similar $\langle l_p^{(k)} \rangle$ values to their linear, flexible chain counterparts. This is because there is no side-chain attached to the $N = 48$ monomer, when $S > 0$, although there is a side-chain attached to the $N = 1$ monomer.

3.4. Fitting the Persistence Length Plots. As we have discussed above, one can define "persistence length" as[4] $\langle l_p^{(k)} \rangle$, or as the arithmetic mean value of $\langle l_p^{(k)} \rangle$ over all k, or as the average over the plateau region of $\langle l_p^{(k)} \rangle$. More generally, we can look at the persistence length histogram, i.e., the probability $w(l_p^{(k)})$, which we shall discuss later on.

We have previously commented[32] that the greater freedom of the free ends reduce $\langle l_p^{(k)} \rangle$. Hence, if one were not interested in the end effects, the first two definitions may be less relevant. In this case, one could average over the plateau region for middle values of k, which has been observed for various polymers.[32] However, this plateau does not always occur, particularly for the more rigid polymers that were studied in this paper. Because each of these definitions can provide substantially different values, we have reported here the whole plots of $\langle l_p^{(k)} \rangle$.

Schäfer and Elsner have recently calculated a relatively simple, asymptotic scaling form for the excluded volume contribution to the stiffness of linear fully flexible chains in the good solvent via the renormalization group and ϵ-expansion.[8] They have predicted the result,

$$\langle l_p^{(k)} \rangle \approx a\left(\frac{k(N-k)}{N}\right)^{2\nu-1} \qquad (11)$$

where a is a constant, N is the number of monomers, and ν is the swelling exponent.[4,5] This appears to fit the simulation data here quite well (see the $\lambda_{ijk} = 0$ plot in Figure 12) with the apparent value of $\nu = 0.618 \pm 0.002$ (see Table 1).

However, as it is not known how to write a field-theory formulation for a semiflexible homopolymer with a fixed persistence length λ_p (no matter how exactly defined), especially at a finite N, there are no renormalization group results available for the rest of the systems studied here other than the fully flexible linear chain.

For a finite λ_p (which depends on the chemical structure of a homopolymer and its external conditions), one could measure the mean-squared radius of gyration R_g^2 and find the *apparent exponent* of its dependence on the degree of polymerization, N, in a certain range of values for the latter via the law $R_g^2 \sim N^{2\nu}$. As one increases λ_p from a fully flexible case, the apparent exponent ν will change from its value ν_{flex} close to the Flory exponent ν_F (subject to a small finite-N correction) toward the value $\nu_{rod} = 1$ of a rigid rod. Clearly,[4] if λ_p is fixed and $N \to \infty$, we shall recover the statistical behavior of a fully flexible chain with $\nu = \nu_{flex}$. However, if we take $N \to \infty$ and $\lambda_p \to \infty$ so that the latter is of the order

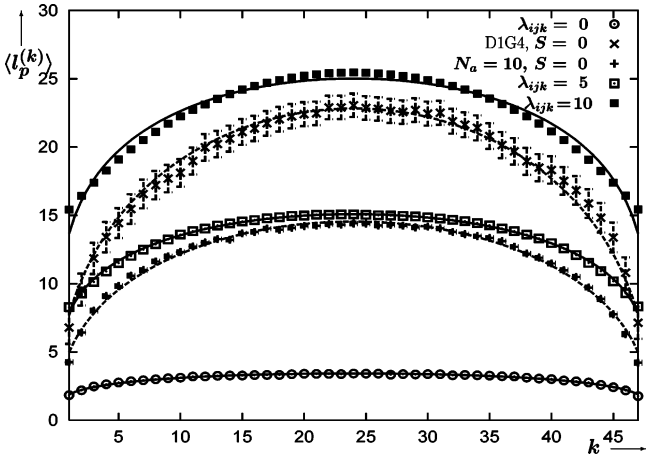

Figure 12. Attempt to fit several of the persistence length plots, $\langle l_p^{(k)} \rangle$, via eq 11. Linear polymers with bending penalties of $\lambda_{ijk} = 0$, 5, and 10, a D1G4 poly(dendron) with $S = 0$ spacers along the backbone, and a comb polymer with arms of length $N_a = 10$ and $S = 0$ spacers were considered. The plotted lines represent the best fits for eq 11.

Table 1: Fitting Parameters for Eq 11 of the $\langle l_p^{(k)} \rangle$ Plots for Various Representative Polymers

polymer	a	ν
Comb Polymers		
$N_a = 5$	3.89	0.694
$N_a = 10$	5.04	0.713
Poly(dendron)s		
D1G1	3.223	0.679
D1G2	4.164	0.691
D1G3	6.294	0.704
D1G4	7.76	0.717
Linear		
$\lambda = 0$	1.90	0.618
$\lambda = 1$	2.96	0.606
$\lambda = 2$	4.19	0.609
$\lambda = 3$	5.51	0.617
$\lambda = 4$	6.68	0.625
$\lambda = 5$	7.90	0.630
$\lambda = 10$ (weak fit)	13.8	0.620

of the contour length of the chain, we also shall obtain the result for a rigid rod, $\nu = \nu_{\text{rod}} = 1$. Thus, the apparent value of ν depends on both λ_p (which is known and fixed for a given polymer under certain external conditions) and N.

Interestingly, although eq 11 was obtained for the intrinsically flexible linear case (i.e., the LCEVC) only, we found reasonable empirical fits for many of the other systems studied here. Fitting parameters for these systems are reported in Table 1 and some of the fits are illustrated in Figure 12. Although the scaling obviously does not account for the steplike behavior observed in $\langle l_p^{(k)} \rangle$ for branched polymers with $S > 0$ (see Figures 10 and 11b), the $S = 0$ branched polymers do seem to be quite well described by eq 11. Indeed, the values of the apparent exponent ν obtained for the comb polymers do have some similarities with values estimated by other means.[32]

As eq 11 does not, strictly speaking, apply to semiflexible polymers, it tends to overemphasize plateaus for middle values of k and to overemphasize the end effects, which are not as dominant for the semiflexible polymers. This is particularly evident for the $\lambda_{ijk} = 10$ plot in Figure 12. Indeed, the best fits that could be obtained for these systems did not demonstrate a substantial increase in apparent ν values with increasing λ_{ijk} (see Table 1), which should take place for more rigid chains[4,5] but only an increase in the prefactor a.

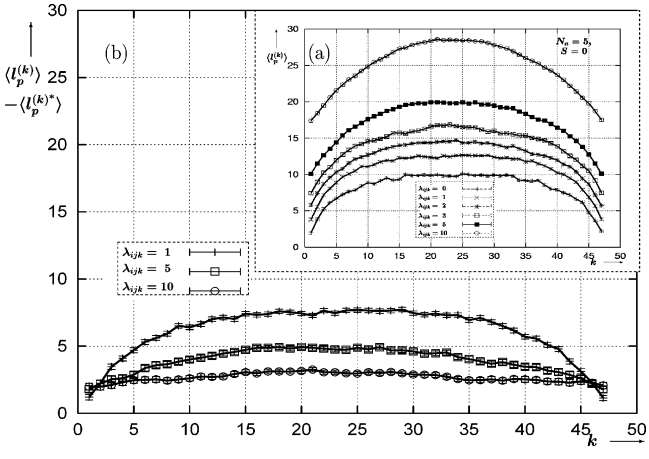

Figure 13. (a) The persistence length plots, $\langle l_p^{(k)} \rangle$, versus segment number, k, as in Figure 10 for comb polymers with $N_a = 5$, $S = 0$ are presented in the inset for increasing values of λ_{ijk} for the monomers in the backbone. In (b), the $\langle l_p^{(k)} \rangle$ plots for the linear, semiflexible polymers in Figure 7 are subtracted from the corresponding plots in (a) for $\lambda_{ijk} = 1$, 5, 10.

3.5. Intrinsically Semiflexible Backbones. For the purpose of distinguishing different types of stiffness, in the previous sections, the branched polymers were assumed to be intrinsically flexible. For the highly branched poly(macromonomer)s, it seems reasonable that a Kuhn length of the polymer could have more than one arm attached.[33] Hence, if one is to characterize these systems more completely, one should include an intrinsic stiffness, as has been done recently.[31,37,38]

Hence, in this section, we will discuss some preliminary results from simulations of comb polymers with intrinsic stiffness. Because this study is limited to the characteristics of the backbone, and to allow a more direct comparison with the other systems that have been studied in this paper, the intrinsic stiffness was only introduced in the backbone.

Figure 13a illustrates the $\langle l_p^{(k)} \rangle$ plots for various comb polymers with $N_a = 5$, $S = 0$, and $\lambda_{ijk} = 0$, 1, 2, 3, 5, 10. With increasing λ_{ijk}, the plots show an increasing similarity to their linear counterparts in Figure 7. This is more obvious if one subtracts the $\langle l_p^{(k)} \rangle$ values of these linear counterparts from the plots in Figure 13a, as has been done for three values of λ_{ijk} (1, 5, and 10) in Figure 13b. It can be seen that the relative contribution of the topological stiffness to the total $\langle l_p^{(k)} \rangle$ plots is somewhat diminished for the more intrinsically stiff combs. Although, even for the $\lambda_{ijk} = 10$ case, the topological stiffness does increase the total stiffness when compared to its linear counterpart in Figure 7.

It is not clear at this stage if this dampening of the total stiffness is due to (a) an actual physical reduction in the topological stiffness, i.e., if the combs are more elongated because of the intrinsic stiffness, then the steric congestion may be less problematic; (b) some sort of saturation effect, whereby the stiffness of the backbone is approaching a maximum (if the persistence length is greater than the length of the backbone); or (c) some other effects. However, from Figure 14, it does appear that the steplike behavior observed in Figure 11 for comb polymers, with $S > 0$ spacers between sidechains along the backbone, is diminished with increasing λ_{ijk}. Indeed, it is not at all apparent for $\lambda_{ijk} = 10$.

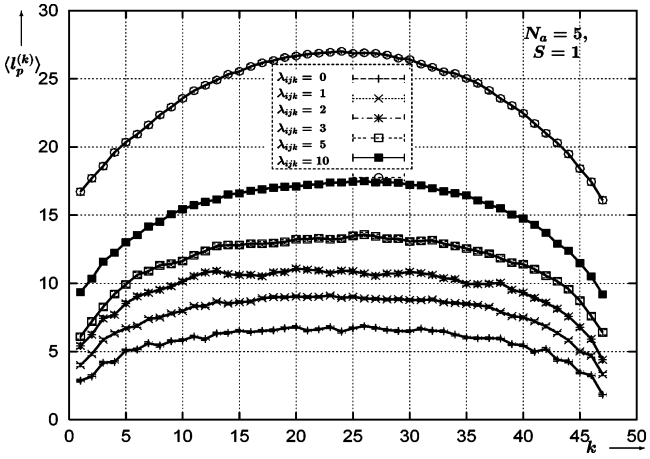

Figure 14. The persistence length plots, $\langle l_p^{(k)} \rangle$, versus segment number, k, as in Figure 10 for comb polymers with $N_a = 5$, $S = 1$, and increasing values of λ_{ijk} for the monomers in the backbone.

Because this steplike behavior is an effect of the topological stiffness, this suggests that the topological stiffness does become reduced somewhat for intrinsically stiff combs.

3.6. $l_p^{(k)}$ Histograms. One can obtain a better understanding of the $\langle l_p^{(k)} \rangle$ plots if one considers their probability distributions, i.e., the histograms, for specific values of k. Figures15 and 16 illustrate these histograms for several different systems, for both $k = 1$ (at the end of the chain) and $k = 24$ (a middle monomer).

Comparing the semiflexible, linear $\lambda_{ijk} = 10$ polymer (Figure 15a) and the D4G2, $S = 0$ poly(dendron) (Figure 15b), one can better understand the similarities and differences previously mentioned in Section 3.3 through an analysis of the histograms. Although the $k = 24$ histograms are quite similar, for the $k = 1$ case, the D4G2 histogram is shorter and broader, leading to a smaller average value of $\langle l_p^{(k)} \rangle$ for D4G2. It appears that the end monomers ($k = 1$) of the semiflexible, linear polymer are more restricted than that of their poly(dendron) counterparts, i.e., their bond vectors are more likely to lie along the direction of the average end-to-end vector, $\vec{R}_b$, i.e., $l_p^{(1)} > 0$. In contrast, the vectors of the end monomers in the poly(dendron) show substantial $l_p^{(1)} < 0$ populations, emphasizing the relatively flexible ends of the poly(dendron)s. However, the $l_p^{(1)} < 0$ population is still substantially smaller than the $l_p^{(1)} > 0$ population, leading to a positive $\langle l_p^{(k)} \rangle$ average (see Figure 8).

In the middle of the poly(dendron), $k = 24$ (see Figure 15b), we find the vectors predominantly lie along the direction of the average end-to-end vector, $\vec{R}_b$, as for the linear semiflexible case (see Figure 15a) with the largest population for $l_p^{(24)} = 30$, suggesting that these vectors are much more restricted, which is not surprising because we have already seen that the backbone is elongated. It should be noted that there is still a significant $l_p^{(24)} < 0$ population for both the poly(dendron) and the semiflexible, linear polymer.

In Figure 16a, we consider a linear polymer with no intrinsic bending penalty, i.e., $\lambda = 0$. If the chain was a totally flexible, random walk, then one would predict identical, symmetric curves for all values of k, with the $l_p^{(k)} < 0$ and $l_p^{(k)} > 0$ populations exactly canceling each other on average, yielding $\langle l_p^{(k)} \rangle = 0$. However, in the good solvent, the excluded volume introduces a bias to the $l_p^{(k)}$ distribution, i.e., the LCEVC. For instance, we notice that the $l_p^{(k)}$ histograms are no longer identical for all k. The $k = 24$ vector is on average more aligned with $\vec{R}_b$ than the $k = 1$ vector, leading to the larger $\langle l_p^{(k)} \rangle$ value for $k = 24$ compared to $k = 1$. Also, we notice that even for the $k = 1$ case, the $l_p^{(1)} < 0$ population is smaller than the $l_p^{(1)} > 0$ population, leading to a positive $\langle l_p^{(k)} \rangle$ average.

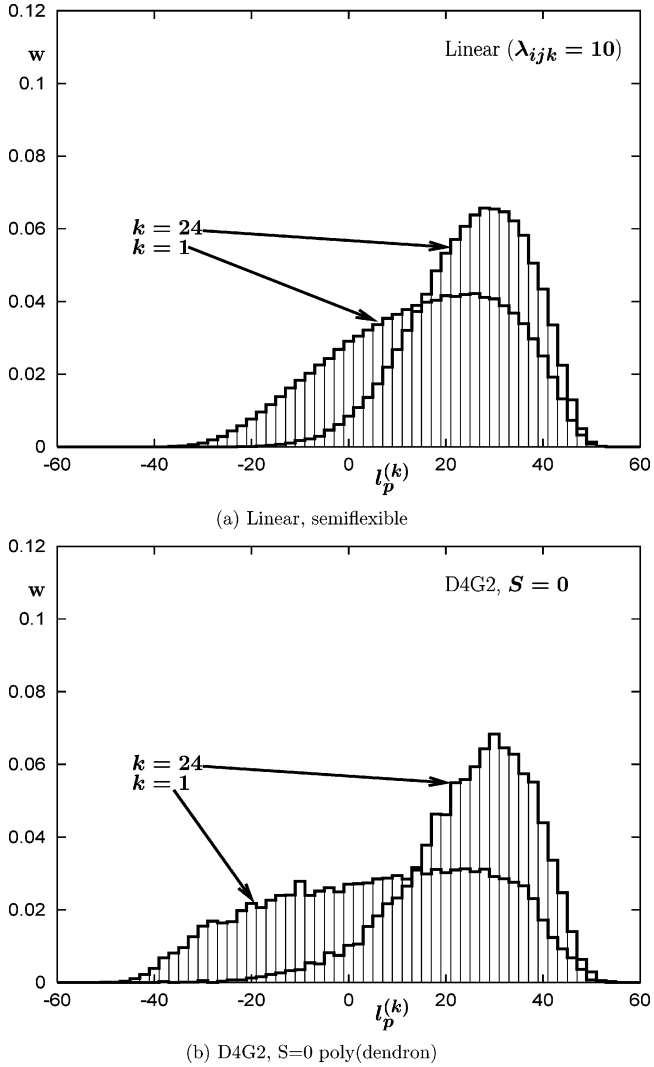

Figure 15. The histograms $l_p^{(k)}$ values (i.e., the probability $w(l_p^{(k)})$) for $k = 1$ and $k = 24$ for (a) the $\lambda = 10$ semiflexible, linear polymer and (b) the D4G2 poly(dendron).

Finally, we note that the $S = 0$ comb polymer in Figure 16b is quite similar to the D4G2 poly(dendron), albeit it appears to be slightly more flexible, e.g., the $l_p^{(24)} < 0$ population is slightly more pronounced for the comb. However, that does not indicate whether poly(dendron)s are stiffer than comb polymers or vice versa, because the $N_a = 10$ arms are less sterically hindering than the D4G2 ($N_{\text{dendron}} = 28$) dendrons.

4. Concluding Remarks

The main aim of this paper was to compare the "topological stiffness" of polymers with side-groups to the "intrinsic stiffness" of linear, semiflexible polymers.

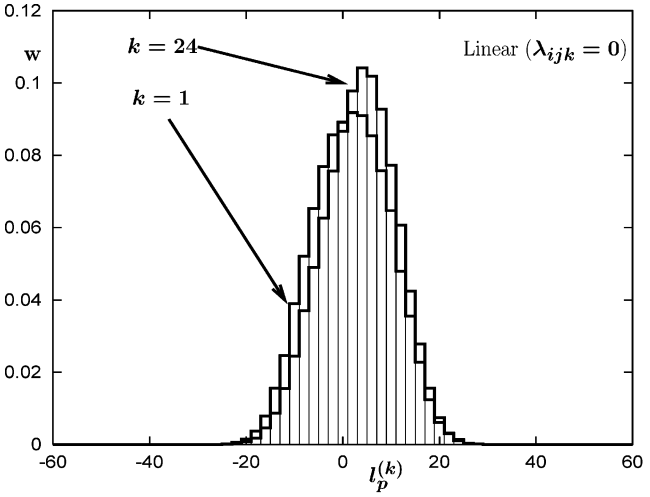

(a) Linear, flexible

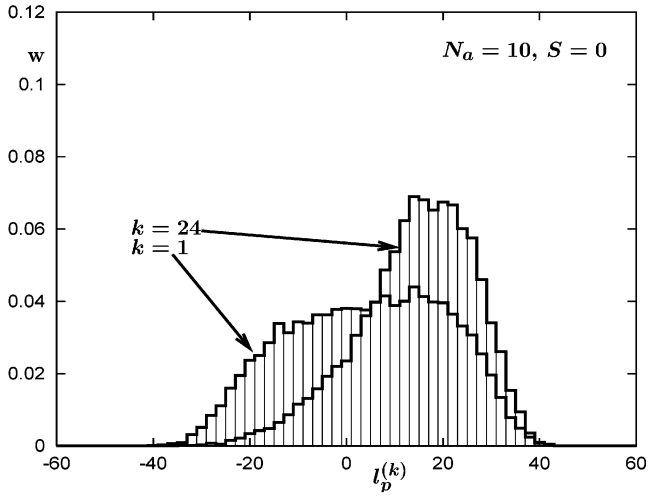

(b) S=0 comb polymer

Figure 16. The histograms of the $l_p^{(k)}$ values for $k = 1$ and $k = 24$ for (a) the $\lambda = 0$, flexible, linear polymer and (b) the $S = 0$, $N_a = 10$ comb polymer with a backbone of length, $N_b = 48$.

This study was carried out because of the current interest in the rigidity of the backbones of polymers that have large numbers of side-chains, but should otherwise be quite flexible. Hence, comb polymers and poly(dendron)s with an intrinsically flexible bead-and-spring model were studied via Monte Carlo simulations in the good solvent. The behavior of the backbones of these branched polymers was then compared to that of linear polymers (of the same length) with various degrees of stiffness introduced by an additional bending penalty term in the model. This bending penalty was used as a model for the intrinsic stiffness of semiflexible polymers. Finally, the behavior of the backbones of branched polymers which also had this bending penalty was considered.

The scattering functions of the various polymers studied here were calculated to allow future comparison with experimental results. The backbones of the "topologically stiff" branched polymers appear to have substantially different scattering behavior to "intrinsically stiff" linear polymers. For instance, for large values of the scattering vector, the branched polymers appeared best modeled as semiflexible polymers, while for smaller values, they appeared better modeled as flexible polymers. This suggests a difficulty in using current simplified scattering models to describe the rigidity of this class of polymer.

The correlation functions of the bond angles formed by the bonds of the backbones as functions of their separation along the backbone were also considered. It was found that the more rigid intrinsically stiff polymers had similar exponential decays to those of Kratky–Porod wormlike chains. However, none of the other systems could be easily modeled by similar exponential decay patterns. We now realize that this is due to the fact that the branched and linear polymers studied here do not have a uniform stiffness along the chain. The Kratky–Porod model assumes an average uniform stiffness, which explains why the more uniformly stiff polymers studied here had some Kratky–Porod behavior.

Because of this difficulty, the systems were also studied via an observable $l_p^{(k)}$, which can illustrate the dependence of the stiffness on the position within the chain, i.e., the projection of the end-to-end vector on the different segment vectors. For the intrinsically stiff, linear polymers, it was found that increasing the bending penalty increases the rigidity of all the vectors in the chain substantially, although the rigidity was greatest in the middle of the chains. For the middle vectors, the topologically stiff backbones showed a similar rigidity to the intrinsically stiff polymers. However, the "end effects" were substantially more pronounced for the topologically stiff polymers, with the end segments appearing quite flexible, something which has experimental relevance.

Interestingly, increasing the number of monomers along the backbone between side-chains resulted in a steplike phenomenon to these plots because of restrictions of the monomers directly connected to the side-chains and their neighbors.

For topologically stiff comb polymers, which also had an intrinsic stiffness in their backbones, it appears that the relative contribution of the topological stiffness to the total stiffness is somewhat diminished, although even for the most intrinsically stiff cases studied here, the topological stiffness appeared to increase the total stiffness.

Finally, to gain a deeper understanding of the end-to-end vector projection plots, the histograms (probability distributions) of $l_p^{(k)}$, were considered for four representative cases. By analyzing these histograms, one can appreciate the subtleties in distinguishing between the traditional description of a polymer's "stiffness" and the different types of restrictions of different segments along the chains. Indeed, for the middle segments, the vectors of both poly(dendron)s and stiff linear polymers lie predominantly along the direction of the end-to-end vector. However, for the end segments, the poly(dendron) vectors have significant probabilities of lying in the opposite direction, leading to an average vector closer to zero.

Acknowledgment. We thank Dearbhla Doyle for her work on gaining preliminary insights into the comb polymer aspects of this study during the course of her undergraduate project. Support from the IRCSET basic research grant SC/02/226 and of the Italian Ministry for Instruction, University, and Research, PRIN2003, is also acknowledged.

References and Notes

(1) Gallacher, L. V.; Windwer, S. *J. Chem. Phys.* **1966**, *44*, 1139.

(2) Lesné, T.; Heroguez, V.; Gnanou, Y.; Duplessix, R. *Colloid Polym. Sci.* **2001**, *279*, 190; Ito, K.; Kawaguchi, S. *Adv. Polym. Sci.* **1999**, *142*, 129; Elias, H.-G. *An Introduction to Polymer Science*, 1st ed.; VCH: New York, 1997.
(3) Denesyuk, N. A. *Phys. Rev. E* **2003**, *67*, 051803; Denesyuk, N. A. *Phys. Rev. E* **2003**, *68*, 031803.
(4) Yamakawa H. *Helical Wormlike Chains in Polymer Solutions*, 1st ed.; Springer-Verlag: New York, 1997; des Cloizeaux, J.; Jannink, G. *Polymers in Solution: Their Modelling and Structure*, Engl. ed.; Clarendon Press: Oxford, 1990.
(5) Doi M.; Edwards, S. F. *The Theory of Polymer Dynamics*, 1st ed.; Clarendon Press: Oxford, 1988.
(6) Kratky, O. In *Small-Angle X-ray Scattering*, 1st ed.; Glatter, O., Kratky, O., Eds.; Academic Press: London, 1982; p 361; Kirste, R. G.; Oberthür, R. C. In *Small-Angle X-ray Scattering*, 1st ed.; Glatter, O., Kratky, O., Eds.; Academic Press: London, 1982; p 387.
(7) Rawiso, M.; Aime, J. P.; Fave, J. L.; Schott, M.; Müller, M. A.; Schmidt, M.; Baumgartl, H.; Wegner, G. *J. Phys. (Paris)* **1988**, *49*, 861; Beaucage, G.; Rane, S.; Sukumaran, S.; Satkowski, M. M.; Schechtman, L. A.; Doi, Y. *Macromolecules* **1997**, *30*, 4158.
(8) Schäfer, L.; Elsner, K. *Eur. Phys. J. B* **2003**, *3*, 0307329; Schäfer, L.; Elsner, K. *Eur. Phys. J. E* **2004**, *13*, 225.
(9) Pedersen, J. S.; Schurtenberger, P. *Macromolecules* **1996**, *29*, 7602.
(10) Ullner, M.; Woodward, C. E. *Macromolecules* **2002**, *35*, 1437.
(11) Barrat, J.-L.; Joanny, J.-F. *Adv. Chem. Phys.* **1996**, *94*, 1; Ha, B.-Y.; Thirumalai, D. *J. Chem. Phys.* **1999**, *110*, 7533; Buhler, E.; Boué, F. *Eur. Phys. J. E* **2003**, *10*, 89.
(12) Micka, U.; Kremer, K. *J. Phys.: Condens. Matter* **1996**, *8*, 9463.
(13) Tsukahara, Y.; Mizuno, K.; Segawa, A.; Yamashita, Y. *Macromolecules* **1989**, *22*, 1546; Tsukahara, Y.; Tsutsumi, K.; Yamashita, Y.; Shimada, S. *Macromolecules* **1990**, *23*, 5201.
(14) Wintermantel, M.; Schmidt, M.; Tsukahara, Y.; Kajiwara, K.; Kohjiya, S. *Macromol. Rapid Commun.* **1994**, *15*, 279; Wintermantel, M.; Gerle, M.; Fischer, K.; Schmidt, M.; Wataoka, I.; Urakawa, H.; Kajiwara, K.; Tsukahara, Y. *Macromolecules* **1996**, *29*, 978; Tsukahara, Y.; Kohjiya, S.; Tsutsumi, K.; Okamoto, Y. *Macromolecules* **1994**, *27*, 1662; Gerle, M.; Fischer, K.; Roos, S.; Müller, A. H. E.; Schmidt, M.; Sheiko, S. S.; Prokhorova, S. Möller, M. *Macromolecules* **1999**, *32*, 2629; Lecommandoux, S.; Chéchot, F.; Borsali, R.; Schappacher, M.; Deffieux, A.; Brûlet, A.; Cotton, J. P. *Macromolecules* **2002**, *35*, 8878.
(15) Wintermantel, M.; Fischer, K.; Gerle, M.; Ries, R.; Schmidt, M.; Kajiwara, K.; Urakawa, H.; Wataoka, I. *Angew. Chem., Int. Ed. Engl.* **1995**, *34*, 1472; Dziezok, P.; Sheiko, S. S.; Fischer, K.; Schmidt, M.; Möller, M. *Angew. Chem., Int. Ed. Engl.* **1997**, *36*, 2812; Djalali, R.; Li, S.-Y.; Schmidt, M. *Macromolecules* **2002**, *35*, 4282; ten Brinke, G.; Ikkala, O. *Trends Polym. Sci.* **1997**, *5*, 213; You, Y.; Hong, C.; Wang, W.; Wang, P.; Lu, W.; Pan, C. *Macromolecules* **2004**, *37*, 7140.
(16) Kaneko, T.; Horie, T.; Asano, M.; Aoki, T.; Oikawa, E. *Macromolecules* **1997**, *30*, 3118.
(17) We note that poly(dendron)s have some similarities with the so-called "dendrigraft" polymers (aka "arborescent" and "comb-burst" polymers), in that these polymers also combine dendritic and linear topologies: Lescanec, R. L.; Muthukumar, M. *Macromolecules* **1991**, *24*, 4892; Teertstra, S. J.; Gauthier, M. *Prog. Polym. Sci.* **2004**, *29*, 277; Tomalia, D. A.; Hedstrand, D. M.; Ferritto, M. S. *Macromolecules* **1991**, *24*, 1438; Gauthier, M.; Möller, M. *Macromolecules* **1991**, *24*, 4548; Gauthier, M.; Li, W.; Tichagwa, L. *Polymer* **1997**, *38*, 6363. However, dendrigraft polymers are dendrimers where polymeric chains are used as the building blocks (rather than smaller monomeric units), while poly(dendron)s comprise a single linear polymeric chain, to which various dendrons are attached.
(18) Grayson, S. M.; Fréchet, J. M. J. *Macromolecules* **2001**, *34*, 6542; Malkoch, M.; Carlmark, A.; Woldegiorgis, A.; Hult, A.; Malmström, E. E. *Macromolecules* **2004**, *37*, 322; Shu, L.; Schäfer, A.; Schlüter, A. D. *Macromolecules* **2000**, *33*, 4321; Fu, Y.; Li, Y.; Li, J.; Yan, S.; Bo, Zh. *Macromolecules* **2004**, *37*, 6395.
(19) Christopoulos, D. K.; Photinos, D. J.; Stimson, L. M.; Terzis, A. F.; Vanakaras, A. G. *J. Mater. Chem.* **2003**, *13*, 2756.
(20) Zhang, A.; Shu, L.; Bo, Zh.; Schlüter, A. D. *Macromol. Chem. Phys.* **2003**, *204*, 328; Frey, H. *Angew. Chem., Int. Ed.* **1998**, *37*, 2180; Schlüter, A. D.; Rabe, J. P. *Angew. Chem., Int. Ed.* **2000**, *39*, 864; Ishizu, K.; Tsubaki, K.; Mori, A.; Uchida, S. *Prog. Polym. Sci.* **2003**, *28*, 27.
(21) Prokhorova, S. A.; Sheiko, S. S.; Möller, M.; Ahn, C.-H.; Percec, V. *Macromol. Rapid Commun.* **1998**, *19*, 359; Prokhorova, S. A.; Sheiko, S. S.; Ahn, C.-H.; Percec, V.; Möller, M. *Macromolecules* **1999**, *32*, 2653; Prokhorova, S. A.; Sheiko, S. S.; Mourran, A.; Azumi, R.; Beginn, U.; Zipp, G.; Ahn, C.-H.; Holerca, M. N.; Percec, V.; Möller, M. *Langmuir* **2000**, *16*, 6862; Sheiko, S. S.; Möller, M. *Chem. Rev.* **2001**, *101*, 4099.
(22) Jahromi, S.; Palmen, J. H. M.; Steeman, P. A. M. *Macromolecules* **2000**, *33*, 577; Ghosh, S.; Banthia, A. K.; Maiya, B. G. *Org. Lett.* **2002**, *4*, 3603.
(23) Yin, R.; Zhu, Y.; Tomalia, D. A.; Ibuki, H. *J. Am. Chem. Soc.* **1998**, *120*, 2678.
(24) Ouali, N.; Méry, S.; Skoulios, A. *Macromolecules* **2000**, *33*, 6185.
(25) Tomalia, D. A.; Kirchoff, P. M. U.S. Patent. 4,694,064, 1987; Kirchoff, P. M.; Tomalia, D. A. Eur. Pat. 0556871, 1993.
(26) Stocker, W.; Schürmann, B. L.; Rabe, J. P.; Förster, S.; Lindner, P.; Neubert, I.; Schlüter, A. D. *Adv. Mater.* **1998**, *10*, 793.
(27) Förster, S.; Neubert, I.; Schlüter, A. D.; Lindner, P. *Macromolecules* **1999**, *32*, 4043.
(28) Schlüter, A. D. *C. R. Acad. Sci., Ser. IIc: Chim.* **2003**, *6*, 843; Percec, V.; Ahn, C.-H.; Ungar, G.; Yeardley, D. J. P.; Möller, M.; Sheiko, S. S. *Nature* **1998**, *391*, 161; Percec, V.; Ahn, C.-H.; Barboiu, B. *J. Am. Chem. Soc.* **1997**, *119*, 12978; Malenfant, P. R. L.; Fréchet, J. M. J. *Macromolecules* **2000**, *33*, 3634; Stocker, W.; Karakaya, B.; Schürmann, B. L.; Rabe, J. P.; Schlüter, A. D. *J. Am. Chem. Soc.* **1998**, *120*, 7691; Karakaya, B.; Claussen, W.; Gessler, K.; Saenger, W.; Schlüter, A.-D. *J. Am. Chem. Soc.* **1997**, *119*, 3296.
(29) For reviews see: Matthews, O. A.; Shipway, A. N.; Stoddart, J. F. *Prog. Polym. Sci.* **1998**, *23*, 1; Grayson, S. M.; Fréchet, J. M. J. *Chem. Rev.* **2001**, *101*, 3819; Bosman, A. W.; Janssen, H. M.; Meijer, E. W. *Chem. Rev.* **1999**, *99*, 1665; Newkome, G. R.; Moorefield, C. N.; Vögtle, F. *Dendritic Molecules: Concepts, Synthesis, Perspectives*; Verlag-Chemie: Weinheim, 1996; Tomalia, D. A.; Naylor, A. M.; Goddard, W. A., III. *Angew. Chem., Int. Ed. Engl.* **1990**, *29*, 138; Mekelburger, H. B.; Jaworek, W.; Vögtle, F. *Angew. Chem., Int. Ed. Engl.* **1992**, *31*, 1571.
(30) Birshtein, T. M.; Borisov, O. V.; Zhulina, Ye. B.; Khokhlov, A. R.; Yurasova, T. A. *Polym. Sci. U.S.S.R.* **1987**, *29*, 1293; Fredrickson, G. H. *Macromolecules* **1993**, *26*, 2825.
(31) Subbotin, A.; Saariaho, M.; Ikkala, O.; ten Brinke, G. *Macromolecules* **2000**, *33*, 3447.
(32) Elli, S.; Ganazzoli, F.; Timoshenko, E. G.; Kuznetsov, Yu. A.; Connolly, R. *J. Chem. Phys.* **2003**, *120*, 6257.
(33) Saariaho, M.; Ikkala, O.; Szleifer, I.; Erukhimovich, I.; ten Brinke, G. *J. Chem. Phys.* **1997**, *107*, 3267.
(34) Saariaho, M.; Szleifer, I.; Ikkala, O.; ten Brinke, G. *Macromol. Theory Simul.* **1998**, *7*, 211.
(35) Rouault, Y.; Borisov, O. V. *Macromolecules* **1996**, *29*, 2605; Shiokawa, K.; Itoh, K.; Nemoto, N. *J. Chem. Phys.* **1999**, *111*, 8165; Khalatur, P. G.; Shirvanyanz, D. G.;, Starovoitova, N. Yu.; Khokhlov, A. R. *Macromol. Theory Simul.* **2000**, *9*, 141; Saariaho, M.; Ikkala, O.; ten Brinke, G. *J. Chem. Phys.* **1999**, *110*, 1180; Sheng, Y.-J.; Cheng, K.-L.; Ho, Ch.-Ch. *J. Chem. Phys.* **2004**, *121*, 1962.
(36) Lipson, J. E. G. *Macromolecules* **1991**, *24*, 1327; Lipson, J. E. G. *Macromolecules* **1993**, *26*, 203.
(37) Saariaho, M.; Subbotin, A.; Szleifer, I.; Ikkala, O.; ten Brinke, G. *Macromolecules* **1999**, *32*, 4439; Saariaho, M.; Subbotin, A.; Ikkala, O.; ten Brinke, G. *Macromol. Rapid Commun.* **2000**, *21*, 110.
(38) Subbotin, A.; Saariaho, M.; Stepanyan, R.; Ikkala, O.; ten Brinke, G. *Macromolecules* **2000**, *33*, 6168.
(39) Metropolis, N.; Rosenbluth, A. W.; Rosenbluth, M. N.; Teller, A. H.; Teller, E. *J. Chem. Phys.* **1953**, *21*, 1087; Allen M. P.; Tildesley, D. J. *Computer Simulations of Liquids*, 1st ed.; Clarendon Press: Oxford, 1987.
(40) Timoshenko, E. G.; Kuznetsov, Yu. A.; Connolly, R. *J. Chem. Phys.* **2002**, *117*, 9050.
(41) Kuznetsov, Yu. A.; Timoshenko, E. G. *J. Chem. Phys.* **1999**, *111*, 3744; Timoshenko, E. G.; Kuznetsov, Yu. A. *Colloids Surf., A* **2001**, *190*, 135.
(42) Millman, R. S.; Parker, G. D. *Elements of Differential Geometry*, 1st ed.; Prentice Hall: New York, 1977.
(43) Carri, G. A.; Marucho, M. *J. Chem. Phys.* **2004**, *121*, 6064.

MA0477246